NANOSYSTEMS:
PHYSICS, CHEMISTRY, MATHEMATICS

Alexeeva O.V., et al. *Nanosystems: Phys. Chem. Math.*, 2025, **16** (6), 919–924.
http://nanojournal.ifmo.ru
DOI 10.17586/2220-8054-2025-16-6-919-924

Original article

Facile synthesis and characterization of FeCoNiPt alloy nanoparticle electrocatalysts with different Pt content

Olga V. Alexeeva[1,a], Olga K. Karyagina[1,b], Sergei S. Kozlov[1,c], Leontiy I. Kuznetsov[1,d], Liudmila L. Larina[1,e], Anna B. Nikolskaya[1,f], Oleg I. Shevaleevskiy[1,d]

[1]N. M. Emanuel Institute of Biochemical Physics RAS, Solar Photovoltaic Laboratory, Moscow, Russia

[a]alexol@yandex.ru, [b]olgakar07@mail.ru, [c]sergeykozlov1@gmail.com, [d]shevale2006@yahoo.com, [e]llarina3333@gmail.com, [f]anickolskaya@mail.ru

Corresponding author: Shevaleevskiy O.I., shevale2006@yahoo.com

ABSTRACT In this work, we present a facile synthesis of FeCoNiPt alloy nanoparticles (NPs) with tunable platinum content (10–30 at.%). The NPs were produced by medium-assisted solid-state reaction using acetylacetonate metal precursors. The structural characterization (TEM, HRTEM, STEM-EDS, and XRD) reveals that the obtained FeCoNiPt NPs exhibit a uniform morphology with an average diameter of 3–7 nm and crystallize in a single-phase face-centered cubic solid solution. Increasing the Pt content leads to lattice expansion and a systematic increase in crystallite size, consistent with the larger atomic radius of Pt. STEM-EDS elemental maps confirm homogeneous incorporation of Fe, Co, Ni, and Pt across individual nanoparticles, demonstrating the successful formation of a multicomponent alloy. This study demonstrates that tuning Pt content in FeCoNiPt multicomponent alloys enables precise modulation of d-band electronic structure. The proposed synthesis approach is simple, cost-effective, and scalable, offering a promising pathway for designing Pt-optimized electrocatalysts.

KEYWORDS nanoparticles, multicomponent alloys, HRTEM, electrodes, electrocatalysis.

ACKNOWLEDGEMENTS The work was carried out within the state assignment of the Ministry of Science and Higher Education of the Russian Federation (theme No. 125020401357-4).

FOR CITATION Alexeeva O.V., Karyagina O.K., Kozlov S.S., Kuznetsov L.I., Larina L.L., Nikolskaya A.B., Shevaleevskiy O.I. Facile synthesis and characterization of FeCoNiPt alloy nanoparticle electrocatalysts with different Pt content. *Nanosystems: Phys. Chem. Math.*, 2025, **16** (6), 919–924.

1. Introduction

The noble metals, including Pt, remain indispensable components of efficient advanced electrocatalysts for hydrogen energy technologies, particularly for the hydrogen and the oxygen evolution reactions [1–7]. However, the high cost and limited availability of Pt significantly restrict its widespread use in large-scale water electrolysis [8–10]. One of the most effective strategies to reduce Pt consumption while maintaining high catalytic efficiency is alloying Pt with Earth-abundant 3d transition metals such as Fe, Co, and Ni. Such alloying lowers the overall precious-metal loading and modifies the electronic structure of Pt, that results in improved catalytic activity through synergistic multimetal interactions [11–14].

Recent studies highlight the exceptional catalytic performance of multicomponent Pt-containing high entropy alloys, including FeCoNiRhPt and FeCoNiTaPt, which exhibit high activity and stability at industrially relevant current densities during water splitting. In line with this, it was shown, that FeCoNiPt alloy exhibits high potential due to its low-cost production possibilities. FeCoNiPt alloy nanoparticles (NPs) can be synthesized using low-temperature chemical routes. It have demonstrated remarkably low HER overpotentials (as low as 11 mV) and mass activities exceeding those of commercial Pt/C by 10–13 times. Thus, one can see high potential of Pt-based multicomponent alloys to be used as efficient and economically feasible electrocatalysts.

A key factor governing the activity of Pt-containing alloys is the electronic structure of the d-band. Alloying induces modifications in several critical parameters, including: the adsorption free energy of hydrogen intermediates, the metal–O–H bond strength governing OER pathways the occupancy and hybridization of d-orbitals, and the position and shape of the d-band centers. Optimizing these d-band characteristics is essential for achieving balanced adsorption energies of HER/OER intermediates, ultimately enhancing catalyst performance.

In this context, FeCoNiPt multicomponent alloy NPs present attractive systems for tuning Pt-centered electronic interactions. The Pt content adjusting makes it possible to regulate the d-band width, orbital overlap, and coordination effects within the alloy lattice. DFT studies predict that a Pt content of approximately 20 % offers an optimal electronic environment, maximizing synergistic interactions while minimizing the amount of Pt used. In this work, FeCoNiPt alloy nanoparticles with controlled Pt contents (10–30 at.%) were synthesized via a simple medium-assisted solid-state reaction [15,16]. Their morphology, crystal structure, elemental distribution, and electrochemical properties were comprehensively

examined. We have shown that the alloy NPs containing ∼20% Pt achieve the most favorable combination of structural uniformity, electronic optimization, and catalytic activity, consistent with the d-band engineering principle. These results provide important insights into the design of multicomponent Pt-based alloys for next-generation electrocatalysts.

2. Experimental

2.1. Synthesis of FeCoNiPt alloy nanoparticles

FeCoNiPt alloy nanoparticles were synthesized using a medium-assisted solid-state reaction, a method previously demonstrated to yield ultrasmall multicomponent alloy nanoparticles with high compositional homogeneity [15]. To synthesize FeCoNiPt alloy NPs, metal acetylacetonate complexes were employed as precursors: iron(III) acetylacetonate ($Fe(acac)_3$), cobalt(III) acetylacetonate ($Co(acac)_3$), nickel(II) acetylacetonate ($Ni(acac)_2$) and platinum(II) acetylacetonate ($Pt(acac)_2$) precursors were used.

To obtain FeCoNiPt nanoparticles with different Pt contents, the total amount of metal precursors was fixed at 1 mmol. Fe, Co, and Ni precursors were introduced in equimolar quantities, while the amount of Pt precursor was varied (0.1, 0.2, and 0.3 mmol), corresponding to targeted Pt contents of approximately 10, 20, and 30 at.%. The precursor mixture was homogenized in an insulating organic medium and subjected to thermal treatment under conditions described previously. After the reaction, the resulting powder was repeatedly washed with organic solvents and purified by centrifugation. The actual elemental compositions of the synthesized nanoparticles were then determined by EDX analysis.

2.2. Materials characterization

The morphology and size distribution of the synthesized NPs were characterized using JEOL 2100F FEG TEM/STEM operated at 200 kV, and JEOL TEM/STEM ARM 200CF equipped with HAADF and annular bright field detectors. High-angle annular dark-field scanning TEM (HAADF-STEM) coupled with energy dispersive X-ray spectroscopy (EDX) was employed for elemental mapping. Selected Area Electron Diffraction patterns were obtained to identify the crystal structure of the NPs. To confirm the structure the d-spacing values were calculated and compared with standard FCC lattice parameters.

3. Results and discussion

3.1. TEM and HRTEM analysis

Transmission electron microscopy confirmed that the FeCoNiPt alloy nanoparticles synthesized using the medium-assisted solid-state reaction exhibit highly uniform morphology and nanoscale dimensions (Fig. 1). The nanoparticles were predominantly spherical and well separated from each other, showing that the synthesis route effectively suppresses agglomeration and enables controlled nucleation and growth. Statistical analysis of particle size shows a narrow distribution centered at 5.31 ± 0.83 nm, that is consistent with the formation of small catalytic grains that may provide enhanced surface reactivity due to their high surface-to-volume ratio that significantly increases the density of exposed active sites.

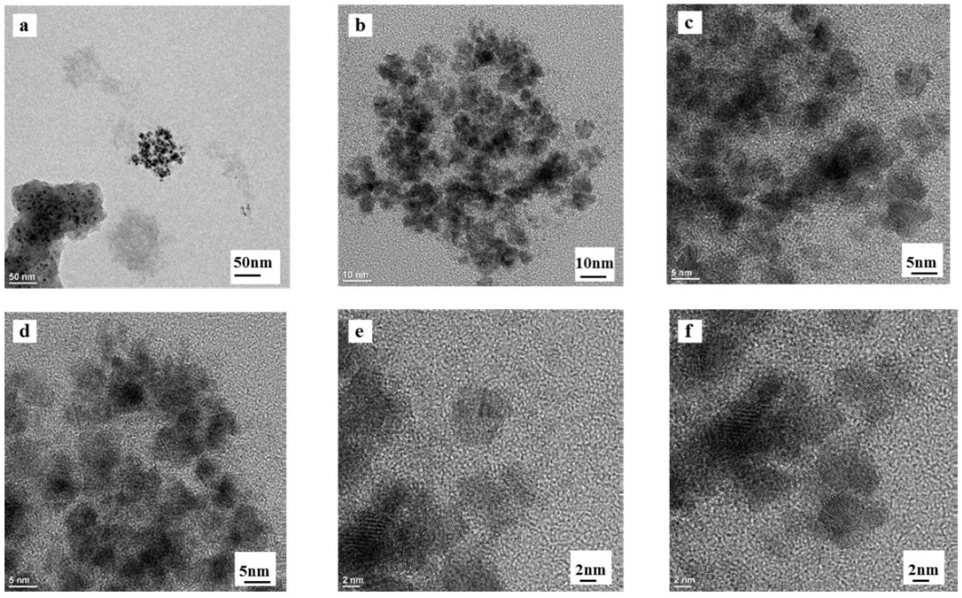

FIG. 1. Transmission electron microscopy (TEM) characterization of FeCoNiPt alloy nanoparticles: high-resolution TEM (HRTEM) images (a, b, c, d) and HRTEM micrographs at higher magnification (e, f).

High-resolution TEM (HRTEM) images show well-dispersed, predominantly spherical FeCoNiPt nanoparticles (Fig, 1: a, b, c, d). Fig. 1 (e, f) presents HRTEM micrographs at higher magnification. It can be seen that high-resolution TEM images display distinct, well-resolved lattice fringes throughout the nanoparticles, confirming their high crystallinity. The presence of continuous and coherent atomic planes suggests that alloying occurs through a homogeneous solid-solution mechanism, with no evidence of core–shell formation, phase separation, or structural defects. The degree of crystalline uniformity is critical for catalytic stability, as grain boundaries and compositional heterogeneities often reduce activity and induce the degradation processes.

3.2. STEM-EDS analysis and quantitative composition of the alloy NPs

High-angle annular dark-field scanning (HAADF) STEM, combined with energy-dispersive X-ray spectroscopy (EDS), was used to evaluate elemental distribution across the nanoparticles. Fig. 2 presents an example of the appropriate data obtained for $Fe_{29.8}Co_{30.2}Ni_{30.6}Pt_{9.4}$ alloy NPs. Z-contrast HAADF images show uniform brightness, implying an even distribution of high- and low-atomic-number elements throughout the sample. As can be seen, elemental mapping confirms that Fe, Co, Ni, and Pt are homogeneously distributed across nanoparticles without detectable segregation and clustering.

The observed compositional uniformity presents a critical characteristic of multicomponent alloys and is essential for achieving synergistic electronic interactions between constituent elements. The formation of a chemically homogeneous alloy ensures that each catalytic site meets similar local bonding environments and enhances the stability of electrocatalytic behavior. Moreover, homogeneous alloying modulates the electronic structure allowing the optimization of adsorption energies for HER and OER processes.

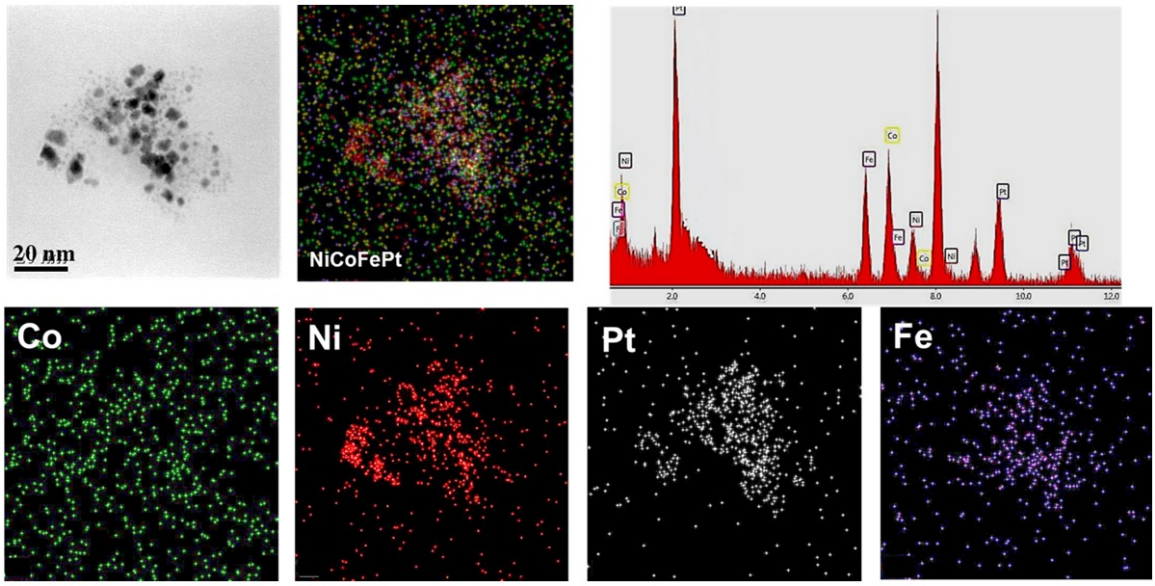

FIG. 2. STEM-EDS elemental mapping of FeCoNiPt alloy nanoparticles. High-angle annular dark-field (HAADF) STEM image of a representative nanoparticles and corresponding elemental maps for Fe, Co, Ni, and Pt.

The combined results of the TEM and STEM-EDS analyses provide strong evidence that the synthesized FeCoNiPt alloy NPs form a single-phase, compositionally homogeneous alloy with ultrasmall particle size. The characteristics obtained are directly relevant for the application in catalysis. Ultrasmall size of NPs ($\sim$5 nm) provides a high density of active surface atoms, homogeneous alloying maximizes synergistic electronic effects among Fe, Co, Ni, and Pt, uniform crystallinity ensures consistent catalytic behavior across particles, while the absence of segregation will prevent the deactivation pathways associated with phase instability. The listed above structural and compositional features will strongly influence the d-band structure of Pt-containing alloys, and enable the possibility of fine-tuning of adsorption strengths for HER and OER intermediates.

The actual elemental compositions of the synthesized alloy NPs determined by EDX analysis and the contents of each element in FeCoNiPt NPs are summarized in Table. The composition of NPs for the initial Pt precursor amount of 10 %, 20 %, and 30 %, was found to be, respectively, $Fe_{29.8}Co_{30.2}Ni_{30.6}Pt_{9.4}$, $Fe_{27.5}Co_{26.7}Ni_{30.6}Pt_{18.7}$, and $Fe_{23.7}Co_{24.3}Ni_{23.8}Pt_{28.2}$. The obtained values correspond closely to the nominal molar ratios used during synthesis, demonstrating reliable incorporation of each precursor into the alloy lattice. Importantly, the agreement between nominal and measured compositions confirms that alloying occurs throughout the nanoparticle volume, not merely at the surface.

TABLE 1. The chemical composition of NPs

Initial Pt precursor amount	Resulted composition of FeCoNiPt NPs (%)			
	Fe	Co	Ni	Pt
10%	29.8	30.2	30.6	9.4
20%	27.5	26.7	27.1	18.7
30%	23.7	24.3	23.8	28.2

The minor deviation in Ni concentration is within typical experimental variation for nanoscale EDS measurements. Critically, the incorporation of all elements in ratios similar to the target stoichiometry confirms that alloying occurs throughout the entire nanoparticle volume, not just at the surface.

3.3. Structural analysis using FFT and SAED

To further elucidate the crystallographic characteristics of the FeCoNiPt nanoparticles, Fast Fourier Transform (FFT) and Selected Area Electron Diffraction (SAED) analyses were carried out. Both techniques provided consistent evidence supporting the formation of a single-phase solid solution with a face-centered cubic (FCC) structure. FFT patterns obtained from several individual nanoparticles exhibit well-defined periodic diffraction spots indicative of ordered atomic arrangements characteristic of the FCC phase (Fig. 3). Inverse FFT (IFFT) reconstruction of selected lattice fringes reveals an interplanar spacing of 0.240 nm, corresponding to the (111) plane of an FCC structure. The average spacing extracted from multiple particles was 0.241 nm, confirming the consistency of the FCC phase throughout the sample. The corresponding lattice parameter, calculated from the (111) spacing, is in good agreement with the expected values for Pt-containing FCC alloys.

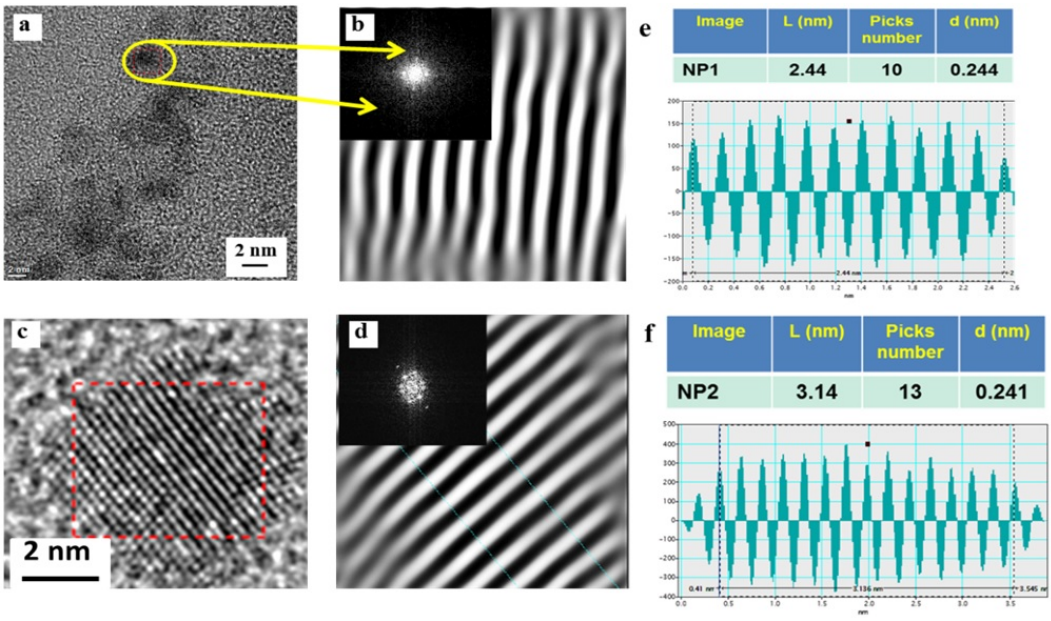

FIG. 3. FFT analysis of representative FeCoNiPt nanoparticles. (a, c) HRTEM images of nanoparticles NP1 and NP2; (b, d) IFFT images showing lattice fringes. In insert: corresponding FFT patterns exhibiting FCC diffraction maxima; (c, e) calculation of the d-spacing values.

The SAED patterns (Fig. 4) display a set of concentric diffraction rings, which can be indexed to the (111), (200), and (200) reflections of an FCC crystal structure. The absence of an additional diffraction rings or discrete spots indicates that the FeCoNiPt nanoparticles crystallize in a single-phase solid solution without detectable secondary phases or elemental segregation. According to SAED measurements the interplanar spacings were found to be: 0.247 nm for (111), 0.219 nm for (200), and 0.162 nm for (220). These values closely match the expected spacings. The excellent agreement between the measured and theoretical values, together with FFT results, confirms that the FeCoNiPt nanoparticles adopt a well-defined FCC phase.

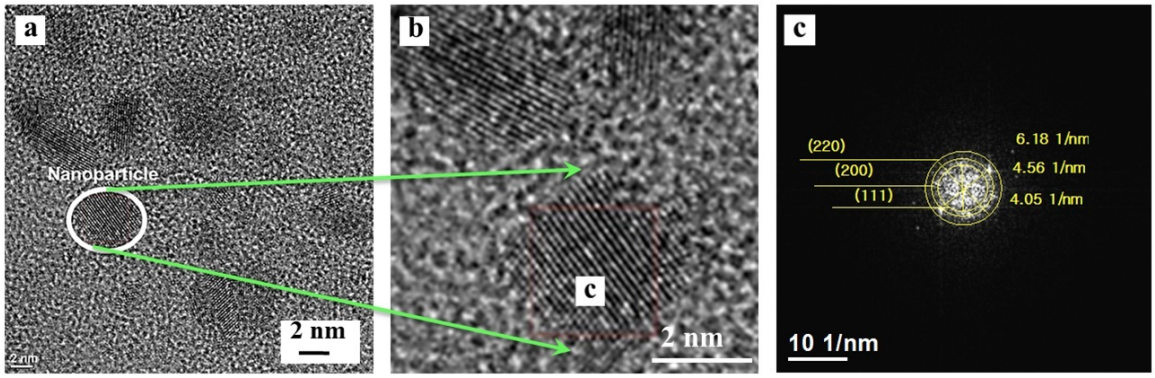

FIG. 4. SAED analysis of FeCoNiPt nanoparticles.(a, b) HRTEM images showing nanoparticle morphology; (c) SAED pattern showing FCC diffraction rings.

3.4. Interpretation of lattice spacing deviations

Minor deviations observed between the experimental and theoretical lattice spacings are expected for multicomponent alloys such as FeCoNiPt. These variations can be attributed to several factors, including atomic-size mismatch between Pt and 3d transition metals; local lattice distortions inherent to multicomponent or high-entropy alloy systems; compositional complexity, including slight differences in the local coordination environment; surface relaxation effects in ultrasmall nanoparticles.

The slightly larger lattice spacing which was observed for the (111) plane (0.247 nm) is consistent with the reported values for other FCC multi-element alloys. In previously reported studies similar d-spacings have been also identified in the range 2.38–2.42 Å for FeNiMnCrCu and 2.35 Å for FeCoNiCrAl. These results demonstrate the stability of FCC structure across a wide compositional range. The agreement between the values obtained in this study and the literature data confirms that the synthesized FeCoNiPt nanoparticles possess a structurally favorable configuration for electrocatalytic activity, which may contribute to their performance in HER and OER.

4. Conclusion

In this work, ultrasmall FeCoNiPt alloy NPs with controlled platinum contents were successfully synthesized using a medium-assisted solid-state reaction. Comprehensive structural and compositional analyses using TEM, HRTEM, FFT, SAED, STEM-EDS, and EDX demonstrate that the obtained NPs form a single-phase, compositionally homogeneous FCC solid solution. The particles exhibit a uniform spherical morphology with a narrow size distribution of $\sim$5 nm, coherent lattice fringes, and an absence of segregation or secondary phases. STEM-EDS mapping confirms the homogeneous incorporation of Fe, Co, Ni, and Pt throughout the nanoparticle volume, verifying the formation of a true multicomponent alloy.

FFT and SAED analyses reveal well-defined FCC diffraction signatures with measured interplanar distances closely matching theoretical predictions. Minor deviations in lattice spacing are attributed to atomic-size mismatch and local lattice distortions typical of multicomponent alloy systems. These features collectively indicate that the alloying process proceeds efficiently, producing structurally stable and electronically interactive FeCoNiPt nanoparticles.

The structural characteristics identified ultrasmall particle size, homogeneous alloying, coherent crystallinity, and lattice strain effects. The listed properties have a direct and beneficial influence on catalytic properties, particularly for electrocatalytic reactions such as the hydrogen evolution reaction (HER) and the oxygen evolution reaction (OER). The observed lattice expansion and uniform multimetal mixing suggest favorable modulation of the electronic structure, including potential tuning of the d-band center, which is a key factor which governs the adsorption energetics on Pt-based alloy surfaces.

Although the present manuscript focuses primarily on synthesis and structural characterization, the demonstrated physico-chemical features strongly suggest that FeCoNiPt alloy NPs are promising candidates for advanced electrocatalytic applications. A detailed investigation of the electrocatalytic performance of FeCoNiPt nanoparticles, particularly towards HER and OER, will be the subject of our next study. The insights obtained here provide a solid foundation for understanding the structure–property relationships that will guide the design of efficient Pt-economized electrocatalysts.

References

[1] Tran D.T., Tran P.K.L., Malhotra D., Nguyen T.H., Duong N.T.A., Kim N.M., Le J.H. Current status of developed electrocatalysts for water splitting technologies: from experimental to industrial perspective. *Nano Convergence*, 2025, **12**, P. 9.

[2] Tahir M., Pan L., Idrees F., Zhang X., Wang L., Zou J.J., Wang Z.L. Electrocatalytic oxygen evolution reaction for energy conversion and storage: A comprehensive review. *Nano Energy*, 2017, **37**, P. 136–157.

[3] Zaman S., Huang L., Douka A.I., Yang H., You B., Xia B.Y. Oxygen reduction electrocatalysts toward practical fuel cells: progress and perspectives. *Angew. Chem. Int. Ed.*, 2021, **60**, P. 17832–17852.
[4] Xiao B., Liu J., Fang J., Zeng J., Liu K., Feng S., Chen J., Lu X.F. Electrospun noble metal-based nanofibers for water electrolysis. *Mater. Chem. Front.*, 2025, **9**, P. 3125–3138.
[5] Wang H., Chen Z.N., Wu D., Cao M., Sun F., Zhang H., You H., Zhuang W., Cao R. Significantly enhanced overall water splitting performance by partial oxidation of Ir through Au modification in core–shell alloy structure. *J. Am. Chem. Soc.*, 2021, **143**, P. 4639–4645.
[6] Reier T., Pawolek Z., Cherevko S., Bruns M., Jones T., Teschner D., Selve S., Bergmann A., Nong H.N., Schlögl R. Molecular insight in structure and activity of highly efficient, Low-Ir Ir–Ni oxide catalysts for electrochemical water splitting (OER). *Am. Chem. Soc.*, 2015, **137**, P. 13031–13040.
[7] Chen H., Guan C., Feng H. Pt-based high-entropy alloy nanoparticles as bifunctional electrocatalysts for hydrogen and oxygen evolution. *ACS Appl. Nano Mater.*, 2022, **5**, P. 9810–9817.
[8] Feng G., Ning F., Song J., Shang H., Zhang K., Ding Z., Gao P., Chu W., Xia D., Sub-2 nm ultrasmall high-entropy alloy nanoparticles for extremely superior electrocatalytic hydrogen evolution. *J. Am. Chem. Soc.*, 2021, **143**, P. 17117–17127.
[9] Guo C., Jiao Y., Zheng Y.. Luo J., Davey K., Qiao S.-Z. Intermediate modulation on noble metal hybridized to 2D metal-organic framework for accelerated water electrocatalysis. *Chem.*, 2019, **5**, P. 2429–2441.
[10] Jin Z., Lv J., Jia H., Liu W., Li H., Chen Z., Lin X., Xie G., Liu X., Sun S. Nanoporous Al–Ni–Co–Ir–Mo high-entropy alloy for record-high water splitting activity in acidic environments. *Small*, 2019, **15**, P. 1904180.
[11] Chuluunbat E., Nguyen A.N., Omelianovych O., Szaniel A., Larina L.L., Choi H.S. Highly electrocatalytic activity of NixFey nanoporous for oxygen evolution reaction in water splitting. *Int. J. Hydrog. Energy*, 2024, **71**, P. 102–109.
[12] Lee G., Nguyen N.A., Nguyen V.T, Larina L.L., Chuluunbat E., Park E., Kim J., Choi, H.S. Keidar M. High entropy alloy electrocatalyst synthesized using plasma ionic liquid reduction. *J. Solid State Chem.*, 2022, **314**, P. 123388.
[13] Nguyen V.T., Lee G.J., Ngo Q.T., Omelianovych O., Nguyen N.A., Trinh V.H., Choi H.S., Mnoyan A., Lee K., Larina L.L., Chen G. Robust carbonencapsulated Ni nanoparticles as high-performance electrocatalysts for the hydrogen evolution reaction in highly acidic media. *Electrochimica Acta*, 2021, **398**, P. 139332.
[14] Ngo Q.T., Omelianovych O., Nguyen V.T., Ahn B.T., Lee K.B., Lee G.J., Larina L.L., Choi H.S. An Economically sustainable NiC catalyst in a solar-to-hydrogen device employing a CIGS submodule. *J. Mater. Chem. A*, 2021, **9**, P. 23828–23840.
[15] Meng C., Wang X., Li Z.,Wu C., Chang L., Liu R., Pei W. Synthesis of FeCoNiCuPt high-entropy alloy nanoparticle electrocatalysts with various Pt contents by a solid-state reaction method. *Materials Advances*, 2024, **5**, P. 719–729.
[16] Chen H., Guan C., Feng H., Pt-based high-entropy alloy nanoparticles as bifunctional electrocatalysts for hydrogen and oxygen evolution. *ACS Appl. Nano Mater.*, 2022, **5**, P. 9810–9817.

Submitted 19 November 2025; revised 29 November 2025; accepted 4 December 2025

Information about the authors:

Olga V. Alexeeva – N. M. Emanuel Institute of Biochemical Physics RAS, Solar Photovoltaic Laboratory, Moscow, Russia; ORCID 0000-0001-8982-3959; alexol@yandex.ru

Olga K. Karyagina – N. M. Emanuel Institute of Biochemical Physics RAS, Solar Photovoltaic Laboratory, Moscow, Russia; ORCID 0000-0002-6702-5195; olgakar07@mail.ru

Sergei S. Kozlov – N. M. Emanuel Institute of Biochemical Physics RAS, Solar Photovoltaic Laboratory, Moscow, Russia; ORCID 0000-0002-8660-5646; sergeykozlov1@gmail.com

Leontiy I. Kuznetsov – N. M. Emanuel Institute of Biochemical Physics RAS, Solar Photovoltaic Laboratory, Moscow, Russia; shevale2006@yahoo.com

Liudmila L. Larina – N. M. Emanuel Institute of Biochemical Physics RAS, Solar Photovoltaic Laboratory, Moscow, Russia; ORCID 0009-0001-5847-6904; llarina3333@gmail.com

Anna B. Nikolskaya – N. M. Emanuel Institute of Biochemical Physics RAS, Solar Photovoltaic Laboratory, Moscow, Russia; ORCID 0000-0002-7430-4133; anickolskaya@mail.ru

Oleg I. Shevaleevskiy – N. M. Emanuel Institute of Biochemical Physics RAS, Solar Photovoltaic Laboratory, Moscow, Russia; ORCID 0000-0002-8593-3023; shevale2006@yahoo.com

Conflict of interest: the authors declare no conflict of interest.